Proc. of IEEE ISWCS 2009, Siena (Italy), pp.498-501, September 7-10, 2009.

Filter Bank Transmission Systems: Analysis with Phase Noise

Nicola Moret and Andrea M. Tonello

Università di Udine
Via delle Scienze 208, 33100 Udine, Italy
phone: (+39) 0432 558042, fax: (+39) 0432 558251
nicola.moret@uniud.it, tonello@uniud.it

***Abstract*—This paper addresses the effect of the phase noise on filter bank modulation systems. We compare the Discrete Multitone (DMT) with the Filtered Multitone (FMT) systems developing an analysis of the distortion due to the Common Phase Error (CPE), the Inter Symbol Interference (ISI) and the Inter Channel Interference (ICI). We consider the *non-coherent* (NCR) and the *coherent receiver* (CR) where the NCR estimates the data symbols without the knowledge of the CPE while the CR assumes perfect knowledge of the CPE.**

I. Introduction

This paper treats the effect of phase noise in transmission systems based on modulated filter banks (FB). In particular, we analyze the DMT (Discrete Multitone) system (also referred to as OFDM [1]) and the FMT (Filtered Multitone) system [2]. They differ in the use the prototype pulses since the DMT system uses a $rect(n)$ pulse, while the FMT system uses a frequency confined pulse, e.g., a $sinc(n)$ pulse.

While the analysis of phase noise has been widely investigated in DMT systems, little work has been done in FMT systems. We present a study of the distortion due to phase noise which includes the effects of the Common Phase Error (CPE) [3], the Inter Symbol Interference (ISI) and the Inter Channel Interference (ICI). The performance is evaluated for both systems considering two types of receivers, the *non-coherent* (NCR) and the *coherent* (CR) receiver. The NCR assumes no knowledge of the CPE, while the CR assumes the knowledge of the CPE.

This paper is organized as follows. In Section II, we describe the system model, and in Section III we report the phase noise model used for the analysis. The evaluation of the CPE in DMT and FMT systems is discussed in Section IV while the ICI evaluation is done in Section V. The theoretical computation of the bit-error-rate (BER) is reported in Section VI, and the numerical results in Section VII. Finally, we report the conclusions.

II. Filter Bank Transmission System

In Fig. 1 we depict the system model considered in this paper. M low rate data signals $a^{(k)}(Nn)$, with $k \in \{0, 1, \cdots, M-1\}$ are upsampled by a factor N then they are filtered with pulses $g^{(k)}(n) = g(n)e^{j\frac{2\pi}{M}kn}$ where $g(n)$ is the prototype pulse, and finally they are summed and transmitted.

The phase noise introduces a multiplicative distortion $\theta(n) = e^{j\phi(n)}$, where $\phi(n)$ is the phase noise, on the transmitted signal $x(n)$. Therefore, the phase noise causes a random phase shift offset on the transmitted signal. We consider a system with an ideal propagation media to better understand the effect of the phase noise.

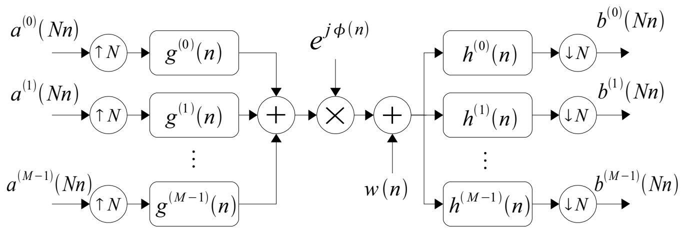

Fig. 1. Generic representation of a Filter Bank scheme, including the phase noise.

The received signal is passed through an analysis FB with pulses $h^{(k)}(n) = g^{(k)^*}(-n)$. The sub-channel outputs of the FB are sampled by a factor N. The output signals are denoted with $b^{(k)}(Nm)$ and can be written as:

$$\begin{aligned} b^{(k)}(Nm) &= \sum_{i=0}^{M-1} \sum_{l \in \mathbb{Z}} a^{(i)}(Nl) \sum_{n \in \mathbb{Z}} g^{(i)}(n - Nl) \\ &\quad \times e^{j\phi(n)}\, h^{(k)}(Nm - n) \\ &= a^{(k)}(Nm)\, G^{(k)}(Nm) + ISI^{(k)}(Nm) \\ &\quad + ICI^{(k)}(Nm) + w^{(k)}(Nm) \end{aligned} \quad (1)$$

where $G^{(k)}(Nm)$ is the equivalent sub-channel response associated to the data of interest.

Therefore, the received sub-channel signal comprises the data symbol multiplied by the gain $G^{(k)}(Nm)$, plus the distortion terms $ISI^{(k)}(Nm)$, $ICI^{(k)}(Nm)$, and the noise $w^{(k)}(Nm)$ component. The ISI and ICI components are a function of both the prototype pulse and the phase-noise process.

It should be noted that in the case of DMT the prototype pulse is rectangular, i.e., $g(n) = rect(n/M)$ where $rect(n) = 1$ for $n \in \{0, \cdots, M-1\}$ and zero otherwise. The ideal FMT system deploys instead the prototype pulse $g(n) = sinc(n/N) = N sin(\pi n/N)/\pi$. For practical applications the Root Raised Cosine (RRC) filter $g(n) = rrcos(n/N)$ is used.

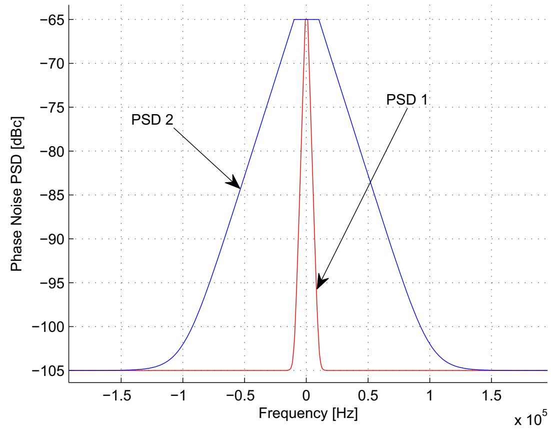

Fig. 2. Phase Noise PSD: PSD1 has $f_1 = 1kHz$, $f_2 = 10kHz$; PSD2 has $f_1 = 10kHz$, $f_2 = 100kHz$. Both have the same parameter $a_\phi = 6.5$, $b_\phi = 4$ and, $c_\phi = 10.5$.

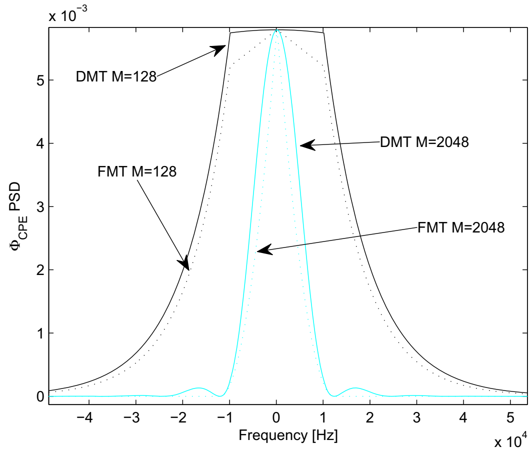

Fig. 3. PSD of the common phase error for $M = 128$ and $M = 2048$ for DMT and FMT systems using the PSD2 phase noise model.

III. Phase Noise Model

In this paper we model the phase noise power spectrum with a general and adaptable model already used in [3], [4] and [5]. This allows describing the phase noise that is introduced by a wide class of commercial oscillators. The power spectral density (PSD) here considered has the following analytic expression

$$R_\phi(f) = 10^{-c_\phi} + \begin{cases} 10^{-a_\phi} & |f| \leq f_{\phi_1} \\ 10^{-(|f|-f_{\phi_1})\frac{b_\phi}{f_{\phi_2}-f_{\phi_1}}-a_\phi} & |f| \geq f_{\phi_1}. \end{cases} \tag{2}$$

The coefficient c_ϕ determines the noise floor, b_ϕ the slope, a_ϕ and f_{ϕ_1} establish the white phase noise region and f_{ϕ_1} is the frequency where the noise floor is dominant. In Fig 2 we report two examples of PSD.

If we assume the standard deviation small enough ($\sigma_\phi << 1$), the term $\theta(n)$ can be rewritten using the Taylor's series expansion as

$$\theta(n) = e^{j\phi(n)} \approx 1 + j\phi(n). \tag{3}$$

The PSD of $\theta(n)$ can then be approximated with:

$$R_\theta(f) = \delta(f) + R_\phi(f). \tag{4}$$

IV. Common Phase Error Analysis

The phase of $G^{(k)}(Nm)$ that we denote with $\Phi_{CPE} = arg(G^{(k)}(Nm))$ is referred to as *Common Phase Error* (CPE) [3] since it is identical on all the sub-channels. It introduces a phase rotation on the transmitted data symbols.

In this paper we present a general framework for the analysis of the CPE, the ISI and ICI components for both DMT and FMT extending the results in [5]. The methodology is general and can be applied to all filter bank transmission systems. Furthermore, our analysis considers the ideal FMT scheme which deploys the $sinc(n/N)$ pulse, but for practical applications a $rrcos(n/N)$ can be used. However, the behavior of the CPE power spectra of the $rrcos(n/N)$ is very close to the $sinc(n/N)$ pulse. The CPE PSD for the case of DMT and ideal FMT systems can be computed in closed form and it is respectively given by:

$$R_{\Phi_E}^{DMT}(f) = (NT)^2\, sinc^2(NTf)\, R_\phi(f) \tag{5}$$

$$R_{\Phi_E}^{FMT}(f) = (NT)^5\, trian^2(NTf)\, R_\phi(f) \tag{6}$$

where we consider a transmitted signal with bandwidth BW and sampling period period $T = 1/BW$.

In Fig. 3 we depict the CPE PSD for both systems assuming $M = 128$ and $M = 2048$ and $N = M$ for both DMT and FMT and using the phase noise PSD_2 in Fig. 2.

V. ICI Power Evaluation

The average power of the ICI component can be computed through the following formula:

$$M_{ICI}^{(k)} = M_a \sum_{\substack{\hat{k}=0 \\ \hat{k}\neq k}}^{M-1} \sum_{l\in\mathbb{Z}} \sum_{\substack{n_1\in\mathbb{Z} \\ n_2\in\mathbb{Z}}} gh^{(k,\hat{k})}(Nl, n_1) r_\theta(n_1 - n_2) \times gh^{(k,\hat{k})^*}(Nl, n_2) \tag{7}$$

where

$$gh^{(k,\hat{k})}(Nl, n) = g^{(\hat{k})}(n - Nl) h^{(k)}(-n) \tag{8}$$

and $r_\theta(n)$ is the correlation of the process $\theta(n)$ directly available applying the inverse Fourier transform on the PSD $R_\theta(f)$.

In Fig. 4, we report the ICI power for DMT and FMT with $N = M$ as a function of the number of sub-channels assuming the phase noise model PSD_2. The figure shows that DMT is somewhat more sensitive to ICI than FMT due to a worse sub-channel spectral containment.

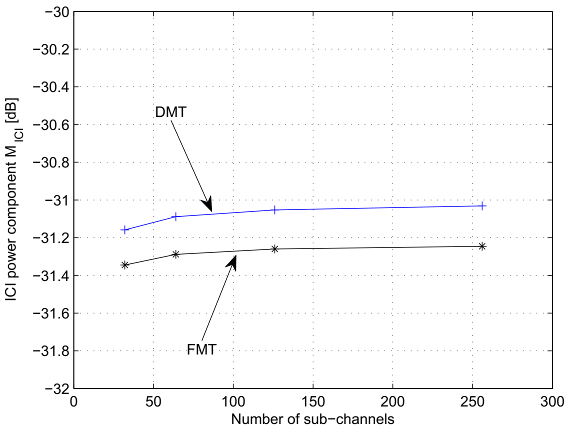

Fig. 4. Power of the ICI components for vs. number of sub-channels for DMT and FMT systems.

VI. Receivers and BER Analysis

We consider both non-coherent and coherent detection. The non-coherent receiver assumes no knowledge of the CPE and uses the following detection metric on each sub-channel:

$$\hat{a}^{(k)}(Nm) = \arg\min_{a\in\mathbb{A}} ||b^{(k)}(Nm) - a||^2 \tag{9}$$

where $\mathbb{A}$ is the constellation alphabet and we assume a unitary energy prototype pulse. For BPSK modulation the error probability $P_e(\Phi_{CPE})$ conditioned on Φ_{CPE} assuming the NCR is

$$P_{e_{BPSK}}(\Phi_{CPE}) = Q\left(\frac{V_0 cos(\Phi_{CPE})}{\sigma_{NI}}\right) \tag{10}$$

with σ_{NI} being the power of the interference plus noise. The average of $P_{e_{BPSK}}(\Phi_{CPE})$ is then:

$$P_{e_{BPSK}} = \int_{-\infty}^{+\infty} Q\left(\frac{V_0 cos(\Phi_{CPE})}{\sigma_{NI}}\right) f_{\Phi}(\Phi_{CPE})\, d\Phi_{CPE} \tag{11}$$

with $f_{\Phi}(\Phi_{CPE})$ being the probability density function of Φ_{CPE}.

Since Φ_{CPE} is a sum of several components it can be approximated as a Gaussian random variable with zero mean and $\sigma^2_{\Phi_{CPE}} = \int_{-B/2}^{B/2} R_{\Phi_{CPE}}(f)df$. Unfortunately, this integral cannot be computed in closed form. An approximation can be obtained if we assume that $\sigma_{\Phi_{CPE}} << 1$. The calculation yields

$$\begin{cases} P_{e_{BPSK}} \approx \frac{1}{\pi}\sigma_{\phi} e^{-SINR/2} \\ SINR = \frac{1}{1/SIR + 1/SNR} \end{cases} \tag{12}$$

where

$$SIR = \frac{E[|a^{(k)}|^2]}{E[|ISI^{(k)} + ICI^{(k)}|^2]} \tag{13}$$

is the signal-to-interference ratio and

$$SNR = \frac{E[|a^{(k)}|^2]}{E[|w^{(k)}|^2]} \tag{14}$$

is the signal-to-noise ratio.

For $QPSK$ modulation the BER with the non-coherent receiver is given by

$$P_{e_{QPSK}} = \frac{1}{2}(1 - (1 - P_{e_{BPSK}})^2). \tag{15}$$

The coherent receiver uses instead the following decision metric under the assumption of knowing the CPE

$$\hat{a}^{(k)}(Nm) = \arg\min_{a} ||b^{(k)}(Nm) - G^{(k)}(Nm)a||^2. \tag{16}$$

Assuming that the CPE varies slowly w.r.t. the prototype pulse length, and that $G^{(k)}(Nm)$ has unitary power, the BER can be approximated as

$$P^c_{e_{BPSK}} = Q\left(\sqrt{2SINR}\right). \tag{17}$$

For $QPSK$ modulation the BER is given by

$$P^c_{e_{QPSK}} = \frac{1}{2}(1 - (1 - P^c_{e_{BPSK}})^2) \tag{18}$$

VII. Numerical Results

Simulation results are reported to evaluate the bit-error-rate performance of both DMT and FMT and compare them with the theoretical analysis. We assume a bandwidth $BW = 25MHz$ with $M = 64$ sub-channels. The interpolation-sampling factor is $N = M$.

First, we report in Fig. 5 and Fig. 6 the results of the theoretical analysis that assumes an FMT system with a $sinc$ prototype pulse. The performance of FMT is worse than that of DMT for high SNRs. The coherent receiver yields improved performance in both systems. The two phase noise PSD models yield essentially the same theoretical performance.

Now, in Fig. 7 and Fig. 8 we report the results obtained via computer simulations. The FMT prototype pulse $g(n)$ is a square-root raised cosine pulse with roll-off $\rho = 0.2$ and extension $L_f = 12N$. We assume $QPSK$ modulation.

The simulations show that the DMT and FMT systems have very similar performance. The CR can correct the distortion due to the CPE therefore it yields better performance than the NCR. In general the ICI component in FMT is smaller that in DMT due to a better sub-channel spectral containment, as it is also shown in the example of Fig. 4. The FMT system also experiences ISI which can be mitigated with sub-channel equalization and this would improve its performance.

Finally, we point out that the BER analytical results approximate reasonably well the simulation results.

VIII. Summary and Conclusion

In this paper we have analyzed the effect of the phase noise on filter bank transmission systems. In particular, we have considered the DMT and the FMT systems and reported a general analysis of the distortion due to the CPE, the ISI and ICI. We have compared the performance of these systems considering the *non-coherent* and the *coherent receiver* where the first receiver assumes no knowledge of the CPE, while the second receiver assumes it perfectly known. Both the theoretical results and the simulation results show that in

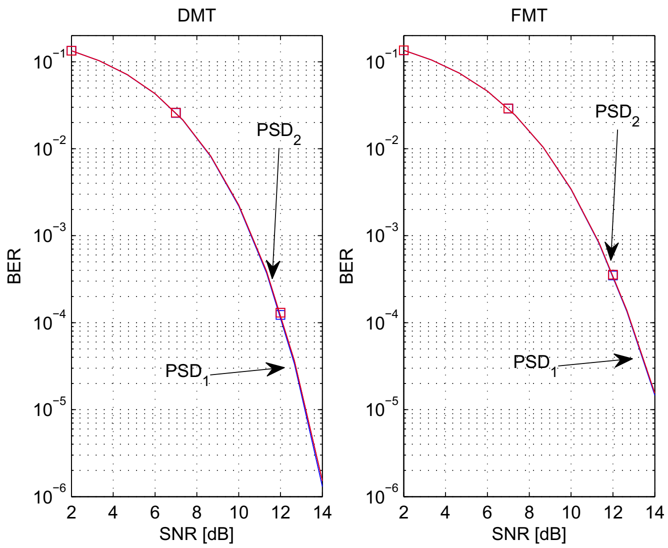

Fig. 5. BER theorical using Eq. (12) for $M = 64$ and $M = N$ with the non-coherent receiver.

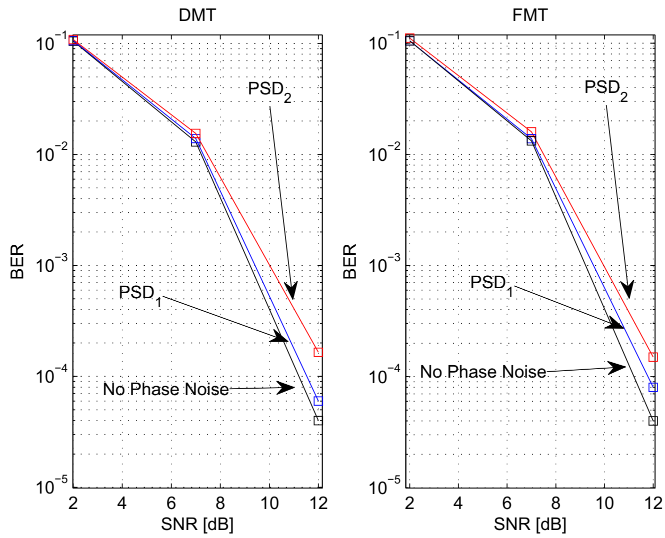

Fig. 7. BER simulated for $M = 64$ and $M = N$ with the non-coherent receiver.

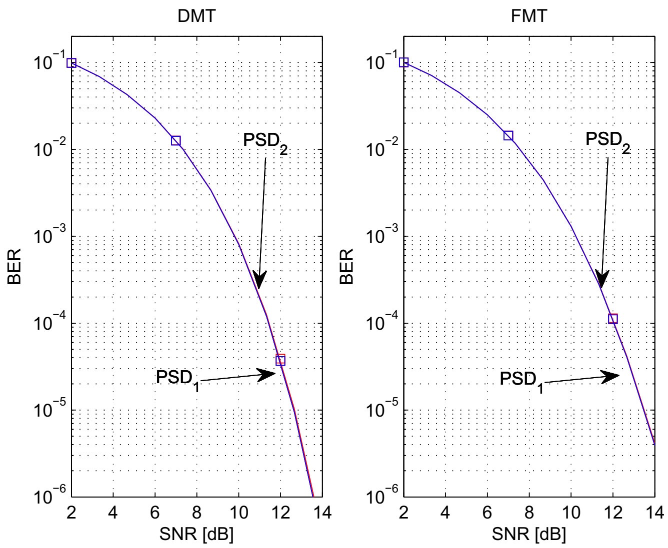

Fig. 6. BER theorical using Eq. (18) for $M = 64$ and $M = N$ with the coherent receiver.

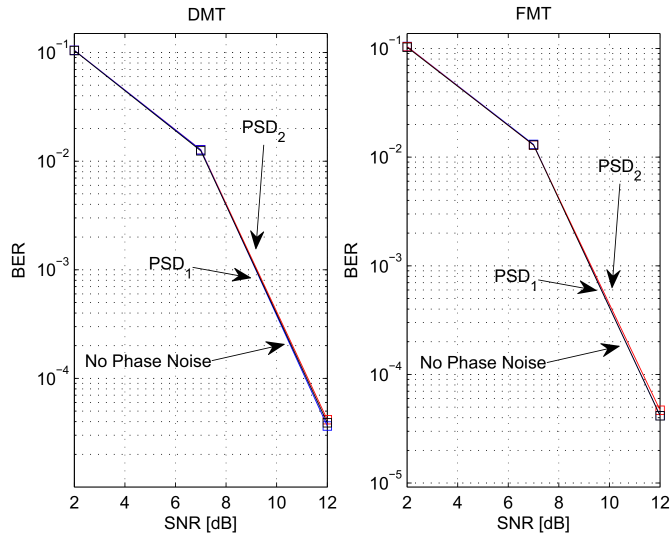

Fig. 8. BER simulated for $M = 64$ and $M = N$ with the coherent receiver.

general DMT and FMT have similar performance with both receivers. Since the FMT system can also exhibit some ISI, its performance can be improved with sub-channel equalization.

ACKNOWLEDGMENT

The work of this paper has been partially supported by the European Communitys Seventh Framework Programme FP7/2007-2013 under grant agreement n. 213311, project OMEGA-Home Gigabit Networks.

REFERENCES

[1] S. Weinstein, P.Ebert *"Data Transmission by Frequency-Division Multiplexing Using the Discrete Fourier Transform"* Communication Technology, IEEE Transactions on Volume 19, Page(s):628 - 634, Issue 5, October 1971

[2] G. Cherubini, E. Eleftheriou, S. Olcer, *"Filtered multitone modulation for very high-speed digital subscribe lines"* IEEE JSAC, pp. 1016-1028 , June 2002.

[3] P. Robertson, S. Kaiser, *"Analysis of the effect of Phase-Noise in Orthogonal Frequency Division Multiplex (OFDM) System"*, pp.1652-1657, In Proc. IEEE ICC'95, Seattle, June 18-22, 1995.

[4] L. Piazzo, P. Mandarini *"Analysis of Phase Noise Effects in ODFM Modems"*, IEE Trans. on Comm., vol. 50, pp. 1696-1705, Oct. 2002

[5] A. Assalini, S. Pupolin, A.M. Tonello, *"Analysis of the Effect of Phase Noise in Filtered Multitone (FMT) Modulated System"*, pp.3541-3545, Proc. of IEEE Globecom 2004, Dallas, Nov.29 - Dec. 3, 2004.